Polymer 51 (2010) 3879–3886

Contents lists available at ScienceDirect

Polymer

journal homepage: www.elsevier.com/locate/polymer

Synthesis of structured nanoparticles of styrene/butadiene block copolymers via RAFT seeded emulsion polymerization

Renzhong Wei, Yingwu Luo*, Zhengshang Li

The State Key Laboratory of Chemical Engineering, Department of Chemical and Bioengineering, Zhejiang University, Hangzhou 310027, China

ARTICLE INFO

Article history:
Received 19 March 2010
Received in revised form
12 May 2010
Accepted 10 June 2010
Available online 18 June 2010

Keywords:
Nanostructured particle
RAFT polymerization
Miniemulsion polymerization

ABSTRACT

The structured nanoparticles of styrene (St) and butadiene (Bd) block copolymers were prepared by RAFT seeded emulsion polymerization of butadiene. It was confirmed that the block copolymers of PSt-b-P(St-co-Bd) was formed with controlled molecular weight and rather low PDI at low composition of the P(St-co-Bd) segment. With more incorporation of butadiene, the branching reaction of polybutadiene became obvious, leading to higher PDI and positive deviation of M_n from the theoretical predication. At the gel point, the composition of the P(St-co-Bd) segment was estimated to be 0.72. After this, the gel fraction increased quickly. The morphology of structured nanoparticles could be largely tuned simply by the copolymer composition. With the composition of the P(St-co-Bd) segment increased from 0.37 to 0.92, the morphology within the structured particles changed from the polybutadiene domains-in-polystyrene matrix, perforated concentric-spherical layer, concentric-spherical multi-layers, bi-continuous, to broken layers of polystyrene in polybutadiene matrix. It was found that the morphology of the block copolymer within nanoparticles was dependent on d/L values, which was in excellent agreement with the theoretical prediction.

1. Introduction

The latex of structured particles has been widely used in many fields of applications like plastic tough modifiers and low volatile organic compound (VOC) aqueous coatings [1]. The structured particles of 50–300 nm are usually composed of two types of polymers usually with large differences in the glass transition temperature. Two types of polymers are phase separated into a length scale comparable to the particle size due to the space confinement of the particles [2,3]. In most cases, the structured particles are used to balance contradictory requirements of material properties. The structured particles were often synthesized by a semi-batch emulsion polymerization process [4]. Tuning the structure of the multiphase particles turned out to be a great challenge since the structure was determined not only by thermodynamic [5–7] but also kinetic factors [8–10]. Important factors include monomer composition, emulsifier and initiator, polymerization temperature, crosslinking, grafting and addition rate of monomers.

Since the middle of 1990s, controlled/living radical polymerization (CLRP) represented by NMP, ATRP and RAFT polymerization has been quickly developed to be powerful tools to synthesize (co) polymer with pre-set molecular weight, narrow molecular weight distribution and well-defined complex chain microstructures like block and gradient copolymer in mild conditions [11–13]. Particularly, CLRP could be carried out in a (mini)emulsion polymerization process [14–19]. Considering that for the block copolymer, a large variety of microphase morphologies of nanometer scales could be obtained and simply tuned by the copolymer compositions, the synthesis of the block copolymer via CLRP in (mini)emulsion would be an interesting facile route to prepare the latex particles with the novel morphologies.

RAFT (mini)emulsion polymerization was intensively investigated in the past decade due to the technological and fundamental interests [20,21]. Considering advantages of the much higher polymerization rate and less termination reactions derived from the compartmentalization effect of (mini)emulsion polymerization than their bulk polymerization counterparts, low viscosity and the water-based green process, RAFT (mini)emulsion polymerization is preferred in the commercial applications of RAFT polymerization. However, both RAFT emulsion and miniemulsion polymerization suffered from the colloidal instability, losing control in molecular weight and its distribution, and low polymerization rate in the early reports [22,23]. Superswelling of a small fraction of the earliest nucleated particles rationalized the colloidal instability, much lower nucleation efficiency than the traditional (mini) emulsion polymerization, the losing control in molecular weight and broadened molecular weight distribution and particle size

* Corresponding author. Fax: +86 571 87951612.
E-mail address: yingwu.luo@zju.edu.cn (Y. Luo).

0032-3861/$ – see front matter © 2010 Elsevier Ltd. All rights reserved.
doi:10.1016/j.polymer.2010.06.023

distribution [24]. A simple equation about the propagating radical number per particle was derived and revealed that the rate retardation was an intrinsic property and could be relieved by the wise selection of the RAFT agent with the low RAFT equilibrium constant [25]. So far, the well controlled RAFT polymerization in both emulsion [26–29] and miniemulsion [30–32] has been achieved in terms of the stable latex, fast polymerization rate, predicted molecular weight and narrow molecular weight distribution.

Few reports dealt with the preparation of the nanostructured particle using CLRP in (mini)emulsion. An interfacial radical miniemulsion polymerization constructed by utilizing the amphiphilic RAFT agent being a surfactant was demonstrated to be an effective route to prepare nanocapsules [21]. The idea was then extended to ATRP systems [33]. The block copolymer synthesized by CLRP in (mini)emulsion polymerization has been documented [30–32,34–36]. However, the morphologies of the block copolymer in the nanoparticles from CLRP in (mini)emulsion were less explored. M. Okubo et al. [35] firstly reported that the "onion-like" multilayered structure was found in the synthesis of the submicron-sized P(*i*-butyl methacrylate)-b-P(styrene) particles by the seeded ATRP in emulsion. The multilayered morphology particles had one layer thickness of approximately 19 nm with the weight ratio of two blocks set to 1/1. B. Charleux et al. [36] investigated the self assembly of P(*n*-butyl acrylate)-b-P(*n*-butyl acrylate-co-styrene) within the latex particles obtained by NMP in emulsion, in which the weigh fraction of P(*n*-BA) block was also set to about 50 wt%. These previous works focused on the effects of the emulsion polymerization process and thermal history on the multilayered nanostructures. The latex particles obtained in the Okubo and Charleux works had the size from 200 nm to 500 nm in diameter. Recently, the morphologies of the block copolymer under nanoconfinement have been theoretically investigated [37,38]. A rich variety of the morphologies were observed, although only the onion-like multilayered structure was observed in the experiment [35,36]. The particle size and the interaction between the component and confining wall were found to strongly affect the equilibrium morphology.

In the current study, we synthesized the block copolymer of styrene and butadiene via RAFT seeded emulsion polymerization of butadiene to prepare the nanostructured latex particles with the varied structures. PSt-b-PBd is a strong segregated system. So, it is easier to tune the morphology by tuning the copolymer composition, compared with the weak segregated systems of polystyrene and polyacrylate or polymethacrylate. A large contrast in the TEM photos could be obtained by stained the residual double bond of PBd, which would help phase observations. Furthermore, the particle size was decreased lower than 200 nm to observe the possible confinement effect on the morphology, which has theoretically been predicted.

2. Experimental

2.1. Materials

De-ionized water (conductivity < 4 μS/cm) was used as received. Styrene was distilled under reduced pressure. Butadiene was distilled directly from a 5-L storage vessel into a cooling steel container. Dicumyl peroxide (DPO, initiator), potassium persulfate (KPS, initiator, >99%), sodium bicarbonate ($NaHCO_3$, pH value buffer, >99%), sodium dodecyl sulfate (SDS, surfactant), hexadecane (HD, co-stabilizer, from Aldrich) were used without further purification. 1-Phenylethyl phenyl dithioacetate (PEPDTA, RAFT agent) with a structure shown in Fig. 1, was synthesized and purified as previously reported [39].

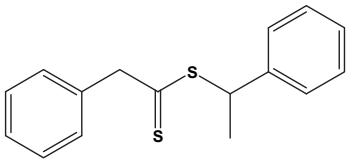

Fig. 1. Chemical structure of the RAFT agent, 1-phenylethyl phenyl dithioacetate.

2.2. RAFT bulk polymerization of butadiene

The mixture of DPO (0.02 g, 7.41×10^{-5} mol) and PEPDTA (0.067 g, 2.46×10^{-4} mol) was transferred into stainless steel tubes. Then, the tubes were subjected to vacuum to remove oxygen. Butadiene (3.0 g, 5.56×10^{-2} mol) was then sucked into the tubes driven by the pressure differences. The tubes were then shaken and stored at 5 °C for 5 h prior to the polymerization to form a homogeneous monomer solution. The polymerization was conducted at 120 °C and the reaction tubes were removed respectively at the pre-set times. The reactions were quenched by cooling the tubes in an ice bath before releasing pressure and then adding 1 mL 0.5 wt% hydroquinone tetrahydrofuran (THF) solution. The polymers were collected by evaporating off THF and the residual monomer.

2.3. Preparation of polystyrene-RAFT seeded latex particles by RAFT miniemulsion polymerization

Styrene (36 g, 0.346 mol) was firstly mixed with HD (1.8 g, 7.96×10^{-3} mol) and PEPDTA (0.47 g, 1.73×10^{-3} mol). This organic mixture was then added to the SDS aqueous solution (3.24 g, 1.13×10^{-2} mol SDS in 264 g water) under gentle stirring for 20 min. The resulted coarse emulsion was subjected to ultrasonication (KS600 sonifier, amplitude 70%, 600 W) for 15 min in an ice-water bath. The obtained miniemulsion was immediately transferred to a 500 ml five-neck flask equipped with a condenser, a thermometer, a nitrogen inlet and a mechanical stirrer. The miniemulsion was stirred at room temperature with highly pure nitrogen purged for 10 min and then immersed in a thermostatic water bath at 70 °C. The addition of KPS (0.15 g, 5.56×10^{-4} mol) and $NaHCO_3$ (0.1 g, 1.19×10^{-3} mol, pH value buffer) dissolved in 3 g water gave the zero time of polymerization. After 150 min of the miniemulsion polymerization (ca. 81% conversion), the latex was cooled down to room temperature as polystyrene-RAFT (PSt-RAFT) seed.

2.4. Preparation of PSt-b-PBd latex particles

The PSt-RAFT seed latex (600 g, 6 wt% solid content), KPS (0.24 g, 8.89×10^{-4} mol) and $NaHCO_3$ (0.16 g, 1.9×10^{-3} mol, pH buffer) were charged into a 1 L autoclave (diameter = 100 mm, height = 180 mm) with a 2-blade skewed propeller (diameter = 50 mm). The autoclave was purged with highly pure nitrogen for 30 min and then was subjected to vacuum. The distilled butadiene (300 g, 5.56 mol) was then pumped into the autoclave. The PSt-RAFT seed particles were swollen by butadiene under gentle stirring for 2 h at room temperature before the polymerization. The polymerization was carried out at 70 °C. The samples were taken via a home-made sampler and quenched by drops of 0.5 wt% hydroquinone aqueous solution after the pressure release. Before sampling, the 10 ml sampler was vaccumized to remove oxygen.

2.5. Characterization

2.5.1. Gel permeation chromatography (GPC) analysis

The molecular weight and molecular weight distribution were determined by GPC (Waters 2487/630C) with three PL columns (10^4,

Table 1
Polymerization of butadiene using PEPDTA in bulk at 120 °C at various times.

Time (h)	Conversion(%)[a]	$M_{n,theo} \times 10^3$	M_n[b] $\times 10^3$	PDI[b]
5	23	3.0	3.6	1.23
10	78	9.5	4.7	1.31
15	92	11.5	7.8	1.35

[a] Determined by gravimetric method.
[b] Measured by GPC analysis by using the universal calibration method with $K_{PSt} = 1.363 \times 10^{-2}$ ml/g, $K_{PBd} = 2.56 \times 10^{-2}$ ml/g, $\alpha_{PSt} = 0.714$,$\alpha_{PBd} = 0.74$ [45–47].

10^3, and 500 Å) and a refractive index (RI) detector. The eluent was THF with a flow rate of 1 mL/min at 30 °C. Molecular weights were calibrated using narrow polystyrene standards (Polymer Laboratory) with molecular weight ranging from 580 to 710,000 g/mol.

2.5.2. Gel content measurement

The copolymers were collected from the latex by precipitation by adding 2 M H_2SO_4, washed out SDS by methanol and dried at 40 °C under vacuum for 5 h. The 0.5 g dried copolymer was dissolved in 100 mL tetrachloride carbon with the moderate agitation for 48 h. The solution was then subjected to filtration and the filtrate was dried until constant weight (w). The gel fraction was calculated by Eq. (1):

$$\text{gel fraction} = \frac{(0.5 - w)}{0.5} \times 100\% \tag{1}$$

2.5.3. Nuclear magnetic resonance spectroscopy (NMR) analysis

Molar compositions of the copolymers were determined by ^{1}H NMR spectroscopy (NMK/300 MHz) in $CDCl_3$ solution (internal reference: tetramethylsilane (TMS), 1wt % solution in $CDCl_3$) at room temperature. ^{1}H NMR signals were assigned as follows (in ppm): 7.15 (2 ortho-H and 1 para-H, $-C_6H_5$ of polystyrene), 6.65 (2 meta-H, $-C_6H_5$ of polystyrene), 5.61 (1H, $-CH{=}CH_2$ of vinyl-1,2 polybutadiene), 5.37(2H, $-CH{=}CH-$ of trans-1,4 polybutadiene), 5.32(2H, $-CH{=}CH-$ of cis-1,4 polybutadiene), 4.92 (2H, $-CH{=}CH_2$ of vinyl-1,2 polybutadiene). The molar ratio of polybutadiene units and polystyrene units was calculated by the ratio of the summation of H signals of $-CH{=}CH-$ of the 1,4 polybutadiene (5.37 ppm, 5.32 ppm) and H of $-CH{=}CH_2$ of the vinyl-1,2 polybutadiene (4.92 ppm) and meta-H signals of $-C_6H_5$ of polystyrene (6.65 ppm).

2.5.4. Differential scanning calorimetry (DSC)

Glass transition temperature (T_g) of the block copolymers were determined by differential scanning calorimetry (DSC) on a TA Instrument equipped with DSC Q100 module. The sample was scanned from −100 to 100 °C with the heating rate of 20 °C min^{-1}. Before the measurement, the thermal history of the sample was removed by heating the sample to 100 °C and holding for 1 min.

2.5.5. Transmission electron microscopy (TEM) observation

The morphology and size of the latex particles were examined by TEM (JEOL, JEM-1230). The samples were prepared as follows: the latex samples were subjected to reduced pressure for 5 h at 40 °C to remove the possible residue monomer and then were diluted to the solid content of 0.005 g/g latex. The dilution was dipped onto the carbon-coated copper grids and dried at room temperature. After 24 h, the TEM samples were stained with RuO_4 vapor at room temperature for 30 min. TEM was operated at 80 kV. The particle sizes were derived from TEM image statistic counting from 300 to 500 particles for each sample. The volume-average particle sizes were calculated from Eq. (2) and the number of particles (N_p,/mL H_2O) was derived from Eq. (3).

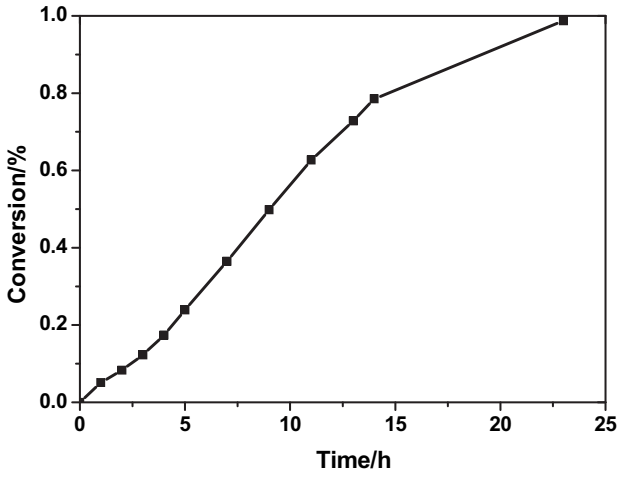

Fig. 2. Kinetic curve of RAFT seeded emulsion polymerization of butadiene at 70 °C.

$$d_v = \sqrt[3]{\sum_{i=1}^{k} n_i d_i^3 \Big/ \sum_{i=1}^{k} n_i} \tag{2}$$

$$N_p = \frac{6[M]_0 x_{con}}{\pi d_v^3 \rho_{poly}} \tag{3}$$

where $[M]_0$ is the initial monomer concentration (g/mL H_2O); x_{con} is the monomer conversion; d_v is the volume-average particle diameter and ρ_{poly} is the density of the polymer. The density of polystyrene and polybutadiene are 1.06 g/ml [40] and 0.88 g/ml, respectively [41]. The density of block copolymers (ρ_{SB}) was calculated by Eq. (4) in the light of their mass composition from ^{1}H NMR data.

$$\rho_{SB} = \frac{m_{SB}}{m_{PSt}/\rho_{PSt} + m_{PBd}/\rho_{PBd}} \tag{4}$$

3. Results and discussion

3.1. RAFT bulk polymerization of butadiene

RAFT solution polymerization of butadiene had been carried out using 2-[(dodecylsulfanyl)carbonothioyl]sulfanyl propanoic

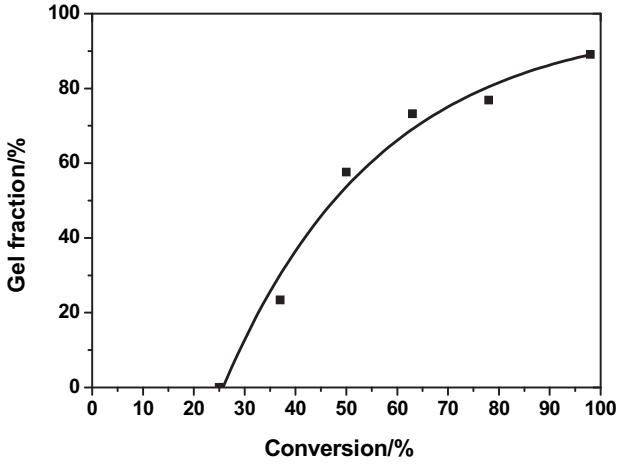

Fig. 3. Gel fraction vs. conversion curve of RAFT seeded emulsion polymerization of butadiene at 70 °C.

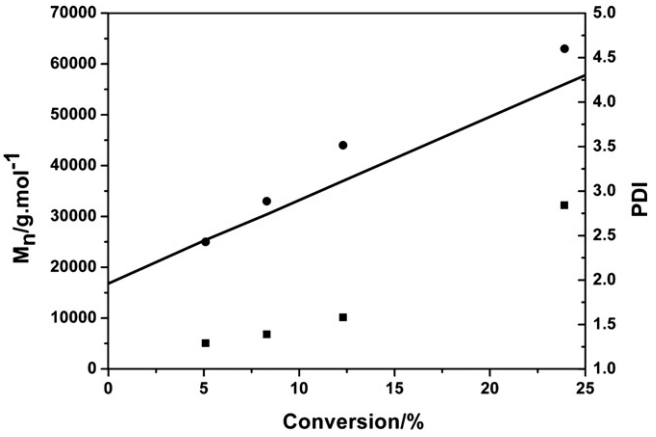

Fig. 4. Evolution of molecular weight (●) and PDI (■) with conversion for RAFT seeded emulsion polymerization of butadiene at 70 °C (—theoretical M_n).

acid as RAFT agent at 60 °C. It was found that the polymerization was not under RAFT control. The synthesis of PSt-b-PBd via the emulsion polymerization was also failed since the butadiene polymerized with little or no molecular weight control within the PSt-RAFT seed particles [34]. In the current paper, PEPDTA was used as RAFT agent, which was an excellent RAFT agent mediating the living radical polymerization of styrene [42]. Since PEPDTA was not used to mediate RAFT polymerization of butadiene yet, the RAFT bulk polymerization of butadiene mediated by PEPDTA was firstly carried out at 120 °C to see if PEPDTA could well control over the polymerization of butadiene. DPO was used as an initiator and the molar ratio of monomer/RAFT/initiator was set to be 225/1/0.33. The results are summarized in Table 1. Molecular weight increases with conversion as predicted. At low conversion, molecular weight is in good agreement with the theoretical prediction. However, at high conversion, molecular weight becomes lower than the theoretical prediction, likely due to the inaccuracy in K_{PBd} and α_{PBd} values. PDIs are quite low but gradually increase from 1.23 at 23% to 1.35 at 92% conversion. The increase in PDI might be ascribed to the irreversible termination due to the quite high initiator level and the possible branching reactions, which are well accepted for butadiene radical polymerization [43,44]. It is clear that PEPDTA is a good mediator for butadiene radical polymerization.

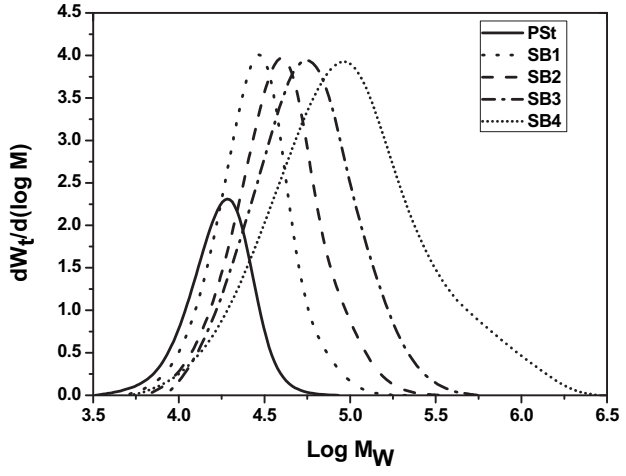

Fig. 5. Evolution of MWDs for RAFT seeded emulsion polymerization of butadiene by PEPDTA at 70 °C.

Table 2
The characteristics of the latexes in RAFT seeded emulsion polymerization.

Samples	Conversion (%)[a]	$M_{th} \times 10^4$	M_n[b] $\times 10^4$	PDI[b]	D_v (nm)[c]	N_p[d] $\times 10^{14}$ (/mL water)
PSt	0	1.68	1.61	1.20	65.8	3.27
SB1	5.1	2.64	2.50	1.29	76.5	3.12
SB2	8.3	3.04	3.30	1.39	88.0	2.43
SB3	12.3	3.70	4.40	1.58	95.9	2.40
SB4	23.9	5.60	6.30	2.84	112.3	2.30

[a] Determined by gravimetric method.
[b] Measured by GPC, relative to PSt standards.
[c] Determined by TEM analysis and eq. (2).
[d] Calculated by eq. (3).

3.2. The seed latex of PSt-RAFT

The seed latex of PSt-RAFT was synthesized via the mini-emulsion polymerization of styrene mediated by PEPDTA with 12% solid content. The polymerization was stopped at 81% conversion. The M_n and PDI of the resulted PSt-RAFT were estimated to be about 16,100 g/mol and 1.2, respectively. Volume-average diameter of the particles removed from the residue monomer was 65.8 nm. From Eq. (5), the dead polymer fraction was calculated to be only 3%, which favors the formation of the block copolymer chains in the following seeded emulsion polymerization.

$$PD = \frac{f_{ini}[I]_0\left(1-e^{-k_d t}\right)}{[RAFT]_0+f_{ini}[I]_0\left(1-e^{-k_d t}\right)} \times 100\% \quad (5)$$

where f_{ini} is initiation efficiency of initiator and $f_{ini} = 0.5$ [48]; $[I]_0$ and $[RAFT]_0$ are the initial concentrations of the initiator and RAFT agent; k_d is decomposition rate constant of initiator and $k_d = 2.33 \times 10^{-5}\ s^{-1}$ [49]. The product latex was then diluted to half of the original solid content as the seed of the butadiene polymerization.

3.3. The seeded emulsion polymerization of butadiene

Fig. 2 presents the polymerization kinetics. It is clear that the polymerization proceeded quite slowly. It took 25 h to finish the polymerization. The low polymerization rate was also found in the conventional seeded emulsion polymerization of butadiene, which was ascribed to the frequent desorption of monomeric radicals derived from the transfer reaction to monomer [50].

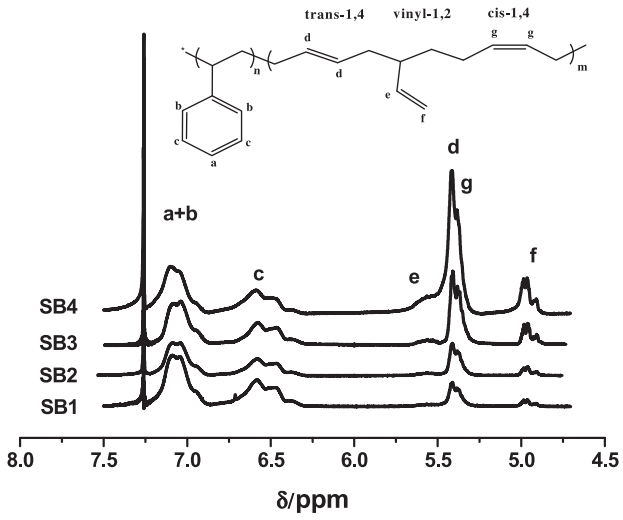

Fig. 6. ^1H NMR spectra between 4.5 and 8.0 ppm in $CDCl_3$ of P(St-b-Bd) copolymers.

Table 3
Composition and $\chi_{eff}N$ of PSt-b-P(St-co-Bd) copolymers before the gel point.

Samples	Copolymer structures[a]	$f_{v,\ P(St\text{-}co\text{-}Bd)}$[a]	$\chi_{eff}N$ (70 °C)[b]
SB1	PSt_{162}-b-$P(St_{38}$-co-$Bd_{96})$	0.37	20.9
SB2	PSt_{162}-b-$P(St_{38}$-co-$Bd_{173})$	0.47	40.3
SB3	PSt_{162}-b-$P(St_{38}$-co-$Bd_{297})$	0.58	73.7
SB4	PSt_{162}-b-$P(St_{38}$-co-$Bd_{647})$	0.72	224.7

[a] Determined by ^{1}H NMR spectroscopy and conversion of styrene.
[b] Calculated by eq. (6).

In the radical polymerization of butadiene, the crosslinking could occur due to the existence of the residue double bond on the polymer chains from butadiene. The gel fraction was monitored during the polymerization. The results are presented in Fig. 3. From Fig. 3, the gel point is estimated to be about 25% conversion. Beyond the gel point, the gel fraction increases quickly.

Four samples were taken before the gel point. Their M_ns and PDIs evolution curves against the monomer conversion are shown in Fig. 4. M_n increases with monomer conversion. At low conversion, M_ns are in good agreement with theoretical prediction. When approaching to the gel point, the experimental M_n becomes larger than theoretical prediction while PDI increases quickly due to the branching reaction. Actually, M_n from GPC, which is relative to polystyrene, would be much lower than the true values near the gel point due to branching structures. From GPC curves shown in Fig. 5, it is clear that the whole GPC curve moves to the higher molecular weight in SB1 and SB2, indicating the formation of the block copolymer. In the cases of SB2, SB3 and SB4, a low molecular weight tail that does not move very much appears, likely due to the formation of some dead polymer. A shoulder peak is clearly seen in the region of high molecular weight ($5.6 < \log M_w < 6.2$) in the case of conversion 23.9%, which is close to the gel point. M_n and PDI are 63,000 g/mol and 2.84, respectively. In the previous bulk polymerization, the PDI is quite low even at very high monomer conversion. The reason is that the target molecular weight is much lower in the bulk polymerization so that the branching degree is quite low even at high monomer conversion [51]. All GPC data of the block copolymer are relative to PSt standards. Castignolles et al. [52] pointed out that such a treatment could mislead. Particularly when the quality of the eluent as a solvent for the standard and the polymer sample is very different, the accuracy of GPC data relative to PSt standards would be very poor. Fortunately, the quality of THF as a solvent is quite similar for PSt and PBd as suggested by their close α values. Additionally, the branching could affect the accuracy of GPC data. However, it is believed the changing trend presented in Fig. 4 should be true.

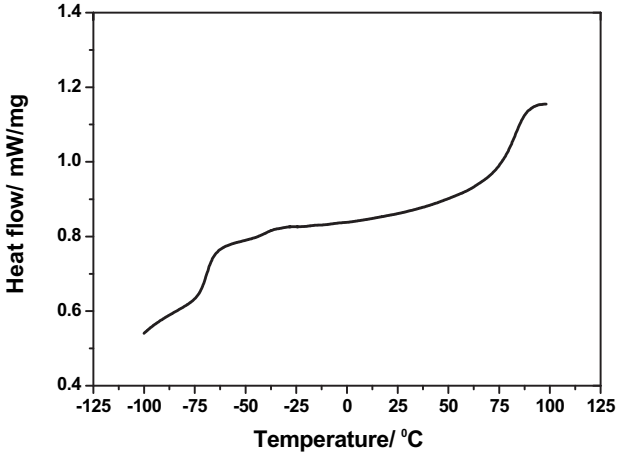

Fig. 7. DSC curve of poly (St-b-Bd) copolymer (sample SB4).

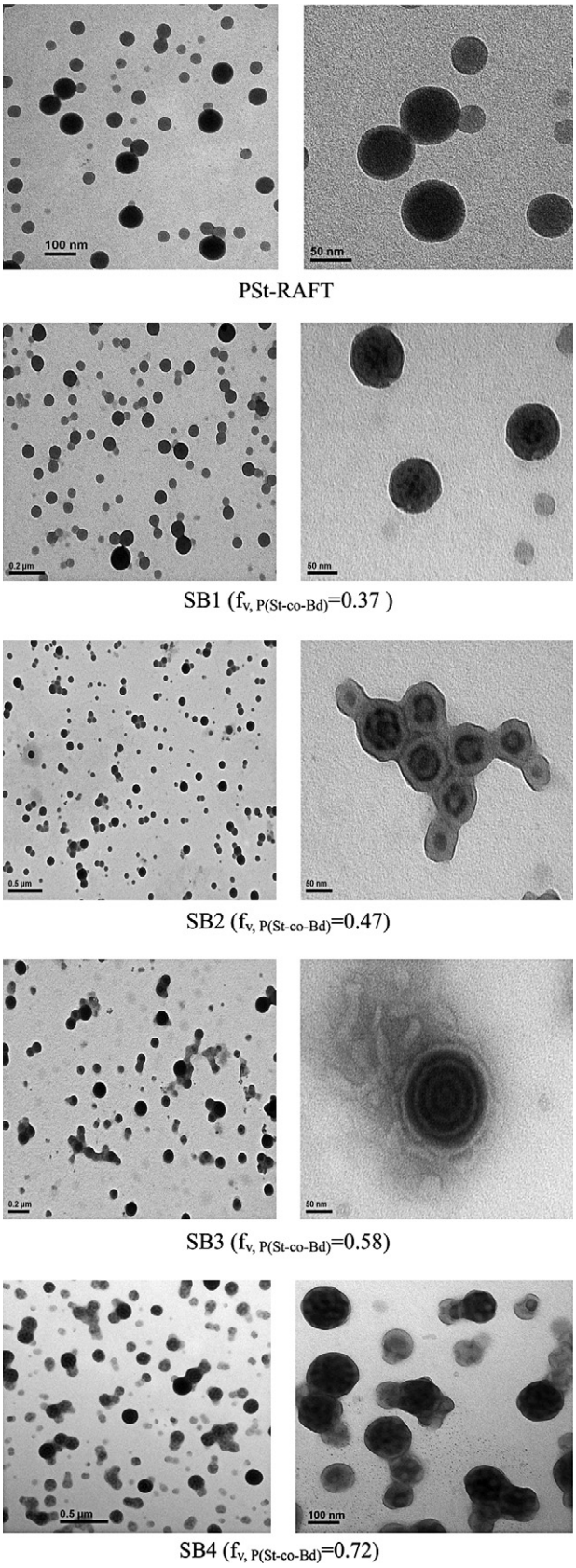

Fig. 8. TEM images of the latex particles before the gel point, stained by RuO_4.

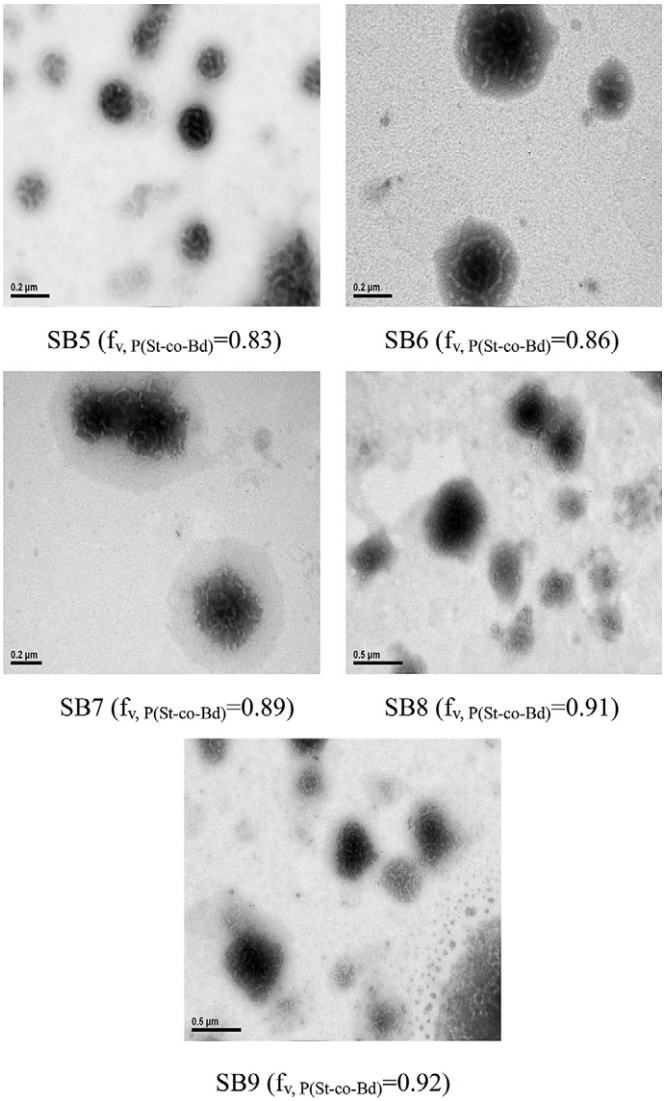

Fig. 9. TEM images of the latex particles after the gel point, stained by RuO_4.

The other characteristics of the latexes before the gel point are listed in Table 2 From N_p data, it seems some degree of aggregation should occur in the early stage of the polymerization. After that, N_p remained constant.

3.4. The composition of the block copolymers

The block copolymer composition of the samples before the gel point was determined by ^{1}H NMR as shown in Fig. 6. The results are listed in Table 3. It was found that the rest of styrene in the seed latex was consumed up at conversion 5.1% derived from conversion and ^{1}H NMR data even though the reactivity ratio of styrene and butadiene are quite close ($r_{St} = 0.78$, $r_{Bd} = 1.39$ at 60 °C). The reason for this is that only a small fraction of butadiene in the reactor could swell the particles, where the polymerization occurred. So, the resulted copolymers actually have a transitional gradient copolymer segment between polystyrene and pure polybutadiene block, which is also evidenced in the glass transition between −50 to −25 °C in the DSC curve as shown in Fig. 7. For simplicity, the transitional segment and polybutadiene block are treated to be one block of the random copolymer of styrene and butadiene in the following discuss and the block copolymer is nominated as PSt-b-P(St-co-Bd). Considering that the fraction of styrene in the polybutadiene block is small, such a treatment should be acceptable. A small fraction of styrene incorporated in the polybutadiene block could decrease the interaction parameter. The effective $\chi_{eff}N$ is determined by the Eq. (6) [53–55]:

$$\chi_{eff}N = \alpha\left(M_{W,PSt}\nu_{PSt} + M_{W,P(St-co-Bd)}\nu_{P(St-co-Bd)}\right)(1-f_{PSt})^2 \quad (6)$$

$$\alpha = -900 + \frac{7.5\times10^5}{T}$$

Table 4
Compositions of PSt-b-P(St-co-Bd) copolymers after the gel point.

Samples	Conversion[a]	$f_{v, P(St-co-Bd)}$[b]
SB5	0.37	0.83
SB6	0.50	0.86
SB7	0.63	0.89
SB8	0.78	0.91
SB9	0.98	0.92

[a] Determined by the gravimetric method.
[b] Derived from the conversion data.

Table 5
Comparisons of theoretically predicted morphology with the TEM observed morphology.

Samples	Morphology in bulk[a]	L[b] (nm)	d[c]/L	Predicted morphology[d]	Morphology from TEM
SB1	HEX	30	2.6	PBd domain-in-PSt matrix	PBd domain-in-PSt matrix
SB2	LAM	33	2–3	concentric-spherical layer	perforated concentric-spherical layer
SB3	LAM	35	4.5	concentric-spherical multi-layers	concentric-spherical multi-layers
SB4	G	/	/	/	G

[a] Determined by modeling phase diagram [58]: HEX is hexagonally packed cylinders, LAM is lamellae and G is bi-continuous phases.
[b] Calculated according to literatures [61,62].
[c] Observed from Fig. 8.
[d] Based on literatures [37,38].

where $M_{W,PSt}$ and $M_{W,P(St\text{-}co\text{-}Bd)}$ are the respective weight-average molecular weights of PSt and P (St-co-Bd); ν_{PSt} and $\nu_{P(St\text{-}co\text{-}Bd)}$ are the respective specific volumes of PSt and P(St-co-Bd); f_{PSt} is molar fraction of polystyrene in the P(St-co-Bd) block and the values of $\chi_{eff}N$ of each block copolymers are listed in Table 3.

Polybutadiene has cis-1,4, trans-1,4 and vinyl-1,2 microstructures, as seen in Fig. 6. From Fig. 6, it is disclosed that the resulted PBd microstructures are the same as that of the conventional radical polymerization (i.e. 34% cis-1,4, 50% trans-1,4, and 16% vinyl-1,2) [56].

From Fig. 7, three obvious glass transition temperatures (T_g) are seen. T_g of PBd block and PSt block are −5 °C and 80 °C, respectively. T_g at −40 °C is assigned to the transitional segment, which is estimated to be −46 °C according to the Fox eq. [57]:

$$\frac{1}{T_g} = \frac{w_{PBd}}{T_{g,PBd}} + \frac{w_{PSt}}{T_{g,PSt}} \tag{7}$$

where w_{PBd} and w_{PSt} are the weight fractions of PBd and PSt in P(St-co-Bd) segment based on the composition of sample SB1. $T_{g,PBd}$ and $T_{g,PSt}$ are the glass transition temperatures of the homopolymers (~−100 °C for PBd and ~100 °C for PSt). It is suggested that the phase separation should occur. Compared with their homopolymers, the T_g values of the block copolymer close up to each other.

3.5. Morphology of the nanostructured particles

PSt-b-PBd copolymers are strongly prone to microphase segregation and show a variety of morphologies dependent on the compositions and molecular weights. The phase diagram of the block copolymer has been well established in the bulk state [58]. More recently, the theoretical simulations have revealed the nano-confinement could exert significant influence on the block copolymer morphology [37,38]. The morphology of PSt-b-P(St-co-Bd) particles sampled at different butadiene conversions were observed with TEM. The change in butadiene conversions offered a convenient way to tune the composition of PSt-b-P(St-co-Bd). The typical TEM images are summarized in Fig. 8 and Fig. 9. From Fig. 8, it is seen that some dark domains appear in the center of particles at 5.1% conversion. The average particle diameter is estimated about 76.5 nm and the dark domain is about 10 nm in size. The block copolymer of this sample is actually PSt-b-P(St-co-Bd), as mentioned previously. The volumetric composition of P(St-co-Bd) segment is about 0.37. According to the composition and $\chi_{eff}N$ value listed in Tables 3 and 4, the bulk morphology of this block copolymer should be lamellar or cylinder. However, the segment of P(St-co-Bd) self-assembles into some nano-domains within the particles. With increase of the chain length of the P(St-co-Bd) segment, some broken dark circles of P(St-co-Bd) with the width about 12 nm appear in those particles of over 50 nm in diameter. The responding morphology might be perforated concentric-spherical layer. However, within those smaller particles, P(St-co-Bd) segment organizes into a dark domain in the center, indicating the significant particle size effects. In the sample SB3, the P(St-co-Bd) composition of the block copolymer reached 0.58. In such a case, the perfect concentric multi-layers of P(St-co-Bd) were observed in those particles as big as about 160 nm. The morphology within the particles looks bi-continuous when further increasing the P(St-co-Bd) segment to 0.72. Further increasing the composition of P(St-co-Bd) segment leads to a phase inversion so that PSt segment becomes a dispersed phase being some broken curved nanolayers as seen in Fig. 9. It is interesting that PSt does not organize into sphere domains (the theoretical morphology) even the composition of P(St-co-Bd) segment is as high as 0.9. It is very likely the crosslinked network of P(St-co-Bd) segment, as indicated by the high gel fraction in these particles (referred to Fig. 3), partly fixed the lamellar morphology formed at lower conversion.

The theory developed by Sundberg and coworkers [5,6] was often used to analyze the resulted morphology within the particles synthesized by traditional emulsion polymerization. The energy of the different morphologies taking the various interfacial energies into account was calculated and the predicted morphology would be the one with the lowest energy. However, the theory of Sundberg cannot be used to predict the morphology of block copolymer since the different polymer chains are covalent-bonded together. Recently, Yu and Chen [37,38] et al simulated microstructures of the bulk lamella-forming A–B (1/1 volume ratio) diblock copolymers and bulk cylinder-forming diblock copolymers confined in spherical nanopores by the Monte Carlo [37] and self-consistent field theory [38]. It was found that the self-assembled morphologies within the spherical nanopores depended strongly on the degree of confinement (represented by the value of d/L, where d was the pore diameter and L was the size of the repeat period in the bulk systems.) and the strength of the interaction between "wall" and the components. In the current cases, the latex particles are a perfect model of the nanopores to show nano-confining effect on the morphology of diblock copolymers as the sizes of particles are less than 200 nm. Compared with polybutadiene, polystyrene should be is a bit more hydrophilic, as indicated from their surface tensions (32 mN/m for PBd [59] and 39.4 mN/m for PSt [60]) though both of them should have a weak interaction with water. Table 5 summarized the theoretical morphologies within the particles as predicted by the model [37,38]. In the cases of SB2 and SB3, the TEM images shown in the Fig. 8 are in excellent agreement with the model predictions. For SB1, the composition is located at the transitional area of the hexagonally packed cylinders (HEX) and lamellae (LAM) in the bulk phase diagram. The dark domain of SB1 shown in Fig. 8-SB1 seems to correspond to the bulk hexagonal morphology. According to the composition of SB4, the bulk morphology was estimated to be bi-continuous. This bi-continuous structure was remained in the nanoparticles, as seen in Fig. 8-SB4 though the theoretical prediction in the nanoparticles is not available yet.

4. Conclusions

The structured nanoparticles of styrene and butadiene block copolymers were prepared by the RAFT seeded emulsion

polymerization. Due to the microphase separation of the block copolymer, the morphologies within the latex particles could be widely tuned by the composition. With the composition of the second segment increased from 0.37 to 0.92, the morphology within the structured particles changed from the PBd domain-in-PSt matrix, perforated concentric-spherical layer, concentric-spherical multi-layers, bi-continuous, to broken layers of PSt in PBd matrix. The morphology of the block copolymer within nanoparticles was dependent on d/L values, indicating a strong nanoconfining effect. Further increasing in the composition of P(St-co-Bd) segment leads to a phase inversion so that PSt segment became a dispersed phase being some broken curved nanolayers. However, PSt did not organize into sphere domains even at $f_{v,\,P(St\text{-}co\text{-}Bd)} = 0.9$, probably due to the earlier-born morphology was fixed by cross-linking. Since the microphases within the particles are fully connected by chemical bond, it is expected that the mechanical properties of the particles should be different from those nanostructured particles by semi-batch emulsion polymerization, which we will evaluate. We expect that the rich morphologies of the latex particles of the block copolymer as firstly presented in the current paper would offer a new avenue in the many application fields like plastics tough modifier and low VOC aqueous coating and adhesive.

Acknowledgements

The authors would like to thank the National Science Foundation of China (NSFC) for Award #20474057, #20774087, #20836007, New Century Excellent Talent in University, Research Fund for the Doctoral Program of Higher Education of China for supporting this research.

References

[1] Broek AD. Prog Org Coat 1993;22:55.
[2] Sundberg EJ, Sundberg DC. J Appl Polym Sci 1993;47:1277.
[3] Chen YC, Dimonie V, El-Aasser MS. J Appl Polym Sci 1992;45:487.
[4] Lee DI. Macromol Chem Macromol Symp 1990;33:117.
[5] Winzor CL, Sundberg DC. Polymer 1992;33:3797.
[6] Winzor CL, Sundberg DC. Polymer 1992;33:4269.
[7] Chen YC, Dimonie V, El-Aasser MS. J Appl Polym Sci 1991;42:1049.
[8] Gonzalez-Ortiz LJ, Asua JM. Macromolecules 1995;28:3135.
[9] Gonzalez-Ortiz LJ, Asua JM. Macromolecules 1996;29:383.
[10] Gonzalez-Ortiz LJ, Asua JM. Macromolecules 1996;29:4520.
[11] Hawker CJ, Bosman AW, Harth E. Chem Rev 2001;101:3661.
[12] Kamigaito M, Ando T, Sawamoto M. Chem Rev 2001;101:3689.
[13] Matyjaszewski K, Xia J. Chem Rev 2001;101:2921.
[14] Nicolas J, Charleux B, Guerret O, Magnet S. Angew Chem Int Ed 2004;43:6186.
[15] Nicolas J, Charleux B, Guerret O, Magnet S. Macromolecules 2005;38:9963.
[16] Yang L, Luo YW, Li BG. Polymer 2006;47:751.
[17] Bowes A, McLeary JB, Sanderson RD. J Polym Sci Part A Polym Chem 2007; 45:588.
[18] Zetterlund PB, Kagawa Y, Okubo M. Chem Rev 2008;108:3747.
[19] Cuningham MF. Prog Polym Sci 2008;33:365.
[20] McLeary JB, Klumperman B. Soft Mater 2006;2:45.
[21] Luo YW, Gu HY. Macromol Rapid Cummun 2006;27:21.
[22] De Brouwer H, Tsavalas JG, Schork FJ, Monteiro MJ. Macromolecules 2000; 33:9239.
[23] Save M, Manguian M, Chassenieux C, Charleux B. Macromolecules 2005;38:280.
[24] Luo YW, Tsavalas J, Schork FJ. Macromolecules 2001;34:5501.
[25] Luo YW, Wang R, Yang L, Yu B, Li BG, Zhu SP. Macromolecules 2006;39:1328.
[26] Luo YW, Cui XF. J Polym Sci Part A Polym Chem 2006;44:2837.
[27] Wang XG, Luo YW, Li BG, Zhu SP. Macromolecules 2009;42:6414.
[28] Save M, Guillaneuf Y, Gilbert RG. Aust J Chem 2006;59:693.
[29] Monteiro MJ, Hodgson M, De Brouwer H. J Polym Sci Part A Polym Chem 2000;38:3864.
[30] Butte A, Storti G, Morbidelli M. Macromolecules 2001;34:5885.
[31] Bozovic-Vukic J, Manon HT, Meuldijk J, Koning C, Klumperman B. Macromolecules 2007;40:7132.
[32] Luo YW, Liu XZ. J Polym Sci Part A Polym Chem 2004;42:6248.
[33] Li WW, Matyjaszewski K, Albrecht K, Moller M. Macromolecules 2009; 42:8228.
[34] Bar-Nes G, Hall R, Sharma V, Gaborieau M, Lucas D, Castignolles P, et al. Europ Polym J 2009;45:3149.
[35] Kagawa Y, Minami H, Okubo M, Zhou J. Polymer 2005;46:1045.
[36] Nicolas J, Ruzette AV, Farcet C, Gerard P, Magnet S, Charleux B. Polymer 2007;48:7029.
[37] Yu B, Li BH, Jin QH, Ding DT, Shi AC. Macromolecules 2007;40:9133.
[38] Chen P, Liang HJ, Shi AC. Macromolecules 2008;41:8938.
[39] Quinn JF, Rizzardo E, Davis TP. Chem Commun 2001;11:1044.
[40] Zoller P, Hoehn HH. J Polym Sci Part B Polym Phys 1982;20:1385.
[41] Weerts PA, German AL, Gilbert RG. Macromolecules 1991;24:1622.
[42] Yang L, Luo YW, Li BG. Acta Polym Sinica 2004;3:462.
[43] Moad G, Rizzardo E, Thang SH. Polymer 2008;49:1079.
[44] Morton M, Salatiello PP. J Polym Sci 1951;6:225.
[45] Meyerhoff G, Appelt B. Macromolecules 1979;12:968.
[46] Meyerhoff G, Appelt B. Macromolecules 1980;13:657.
[47] Xu ZD, Song MS. Macromolecules 1981;14:1591.
[48] Maxwell IA, Morrison BR, Napper DH, Gilbert RG. Macromolecules 1991; 24:1629.
[49] Kolthoff IM, Miller IK. J Am Chem Soc 1951;73:3055.
[50] Verdurmen EM, Dohmen EH, Verstegen JM, Maxwell IA, German AL, Gilbert RG. Macromolecules 1993;26:268.
[51] Wang R, Luo YW, Li BG, Zhu SP. Macromolecules 2009;42:85.
[52] Castignolles P, Guillaneuf Y. J Polym Sci Part A Polym Chem 2008;46:897.
[53] Shibayama M, Hashimoto T, Hasegawa H, Kawai H. Macromolecules 1983; 16:1427.
[54] Han CD, Kim J, Kim JK. Macromolecules 1989;22:383.
[55] Roe RJ, Zin WC. Macromolecules 1980;13:1221.
[56] Condon FE. J Polym Sci 1953;11:139.
[57] Fox TG. Bull Am Phys Soc 1956;1:123.
[58] Matsen MW, Bates FS. J Polym Sci Part B Polym Phys 1997;35:945.
[59] Lee L, Lee H. J Polym Sci Part A Polym Chem 1970;5:1103.
[60] LeGrand DG, Gaines Jr GL. J Colloid Interface Sci 1973;42:181.
[61] Helfand E, Wasserman ZR. Macromolecules 1976;9:879.
[62] Helfand E, Wasserman ZR. Macromolecules 1980;13:994.